Hydrate Formation Using Water Spraying onto a Cooled Solid Surface in a Guest Gas

Sadatoshi Matsuda, Hidehiko Tsuda, and Yasuhiko H. Mori
Dept. of Mechanical Engineering, Keio University 3-14-1 Hiyoshi, Kohoku-ku, Yokohama 223-8522, Japan

DOI 10.1002/aic.10890
Published online June 8, 2006 in Wiley InterScience (www.interscience.wiley.com).

An experimental study has been performed involving water spraying onto a cooled metal-block surface exposed to a hydrate-forming gas as a means of high-rate hydrate formation for the purpose of, for example, natural-gas storage. Special attention has been paid to the effectiveness of conductive cooling through the metal block for directly removing the heat released by the hydrate formation from its site, that is, the surface of the metal block, and, thereby, increasing the rate of hydrate formation. HFC-32 (CH_2F_2) that forms a structure-I hydrate at moderate pressures was used as a model gas to enable visual observations of the hydrate formation inside a large-windowed spray chamber. The experiments revealed that the cooling by the metal block effectively increases the rate of hydrate formation while water is sprayed at a given volumetric rate and at a given degree of subcooling from the guest-gas/water/hydrate equilibrium temperature. © 2006 American Institute of Chemical Engineers *AIChE J,* 52: 2978–2987, 2006
Keywords: clathrate hydrate, gas hydrate, hydrate formation, natural gas storage, energy storage

Introduction

This article reports on an experimental examination of a new, as-yet unestablished hydrate-formation technology, which is possibly applicable to industrial-scale operations of forming hydrates from, for example, natural gas for its storage or from biogases for separating undesirable (toxic or incombustible) species, such as hydrogen sulfide and carbon dioxide, which form hydrates at lower pressures than methane. For such industrial applications involving hydrate-forming operations, we need to establish hydrate-formation technology (including the design of the hydrate-forming reactors and their operational scheme) which ensures a sufficiently high-rate hydrate production per unit reactor volume, and also the compatibility with the scaling-up of the reactors from the laboratory scale to the bench-scale, the pilot-plant scale, and finally the commercial-plant scale. Various types of hydrate-forming reactors have been proposed and tested specifically for developing the hydrate-based technology for natural gas storage. A general overview of reactor designs for hydrate production from natural gas was reported by Mori,[1] specifying the potential advantages and disadvantages of each type of reactor proposed and tested so far on the laboratory to pilot-plant scales. In this article, we focus our attention on the water-spraying type, the type of reactors in each of which liquid water is sprayed in a continuous phase of a hydrate-forming gas (or gases), and describe our attempt at modifying the conventional water-spraying-type design to yield a higher hydrate-forming performance.

In general, there are two conditions that need to be satisfied in order to produce a high rate of hydrate formation: (1) a good mixing of the hydrate-guest gas (the hydrate-forming feed gas) and water, and (2) an effective cooling for removing the heat released by the hydrate formation. (In the case of the structure-H hydrate formation, a good mixing of the three phases — the guest gas, water, and a *large-molecule guest substance* (LMGS)[1, 2] which is typically an oily liquid — is required. However, we do not focus our attention on the structure-H hydrate formation in this article.) The water spraying into the

Correspondence concerning this article should be addressed to Y. H. Mori at yhmori@mech.keio.ac.jp
Current address of S. Matsuda: Chiyoda Corp., 2-12-1 Tsurumichuo, Tsurumi-ku. Yokohama 230-8601, Japan
Current address of H. Tsuda: The Kansi Electric Power Co., Inc., 3-6-16 Nakanoshima, Kita-ku, Osaka 530-8270, Japan.

guest-gas phase well meets condition (1). We also note another advantage of the water spraying technique: the facility for scaling up a hydrate-forming reactor just by multiplying the spray nozzles to be installed in the reactor. On the other hand, the water spraying technique generally conflicts with condition (2), which is the major issue underlying this study.

The water spraying technique for hydrate formation was first demonstrated by Rogers et al.[3] Water was sprayed downward by an ultrasonic atomizer into an ethane gas phase confined in a vertically oriented cylindrical cell with its side wall being cooled from the outside. Obviously, the cooling depending on the spray-to-wall heat transfer should become increasingly ineffective with an increase in the reactor size. In a reactor equipped with multiple spray nozzles, many of the water sprays formed there must inevitably be away from the wall of the reactor, and, hence, they must be minimally cooled. An alternative way of cooling was conceived by two Japanese industrial groups,[4,5] and has been used in laboratory-scale experiments.[2,6–8] Water sprayed and accumulated at the bottom of the reactor was continuously pumped to an external heat exchanger (a heat radiator) to be cooled, then pumped back to the reactor to be sprayed again. The cool energy (that is, the enthalpy deficiency corresponding to the water subcooling before spraying, $\Delta T_{\mathrm{sub},\,w}$, measured from the gas/water/hydrate three-phase equilibrium temperature T_{eq}) conveyed by the circulating water to the reactor could compensate for the heat released by the hydrate formation. This way of cooling should function regardless of the reactor size as long as the rate of water circulation is varied in proportion to the capacity of the reactor (the expected rate of hydrate production by the reactor). However, the cooling capacity per unit water flow rate is limited by the risk of obstructing the water-circulation loop due to hydrate formation, which increases with an increase in $\Delta T_{\mathrm{sub},\,w}$. (The possible mechanism of hydrate formation in the loop is explained in some detail elsewhere.[1]) Thus, in order to ensure a sufficient cooling capacity, the water flow rate through the loop must be maintained at an excessively high-level compared to the rate of water consumption due to the hydrate formation, using a large pumping power.

An idea, which possibly overcomes the above difficulty in the cooling of water-spray-type hydrate-forming reactors, was provided by Fukumoto et al.,[9] but it still requires careful examination for its practical utility. The idea was to utilize the impingement heat transfer from sprayed water to the surface of a cooled, highly heat-conductive slab (or block). The slab may be embedded in the wall of a reactor such that its front surface is exposed to the guest gas while its backside is steadily chilled. Alternatively, the slab may be an internally tubed *cold plate* vertically hung into the reactor such that both sides of it are exposed to the guest gas. Water is sprayed from a horizontally oriented spray nozzle (or nozzles) such that water droplets impinge almost vertically on the surface of the cooled slab. If hydrate formation occurs on the surface, the heat released there should directly be removed by heat conduction into the slab. Using a cooled copper block with its front side extruded into a spray chamber charged with HFC-32 (CH_2F_2), a structure-I hydrate forming gas, Fukumoto et al.[9] observed the hydrate formation which resulted in the growth of a hydrate layer sticking onto the surface of the block. Because of the insufficient space beneath the block inside the chamber, the block surface was buried in a pile of the formed hydrate within a short time (typically several minutes) after hydrate nucleation. Thus, the utility of the impingement cooling scheme is yet-to-be clarified.

This study was aimed to test the utility of the impingement cooling scheme, and to examine its effectiveness on hydrate formation. A spray chamber for forming a hydrate was newly designed and constructed, based on the experience obtained in the preceding study of Fukumoto et al.[9] Following the preceeding study, HFC-32 that forms a structure-I hydrate at moderate pressures was used as the model gas for the convenience of visual observations of the hydrate formation inside the spray chamber. Inside the chamber, a spray nozzle faced the front surface of a metal block, the rear of which was extruded out of the chamber and exposed to a jet of liquid coolant (an aqueous ethylene glycol solution). The operational parameters that we varied in this study were the pressure inside the chamber, the temperature of water just before spraying, and the temperature of the coolant for cooling the metal block. Throughout each experimental run, we continuously measured the rate of the HFC-32 supply to the chamber and the heat-flow rate through the metal block to the outside of the chamber in order to estimate the rate of HFC-32 consumption due to hydrate formation, and to evaluate the role of the cooling via the block in the observed hydrate formation, respectively.

Description of Experiments

Experimental apparatus

Figure 1 shows the major portion of the experimental apparatus used in this study. It is a spray chamber integrated with a few auxiliary assemblies. The spray chamber itself was composed of two parts separately machined from stainless steel: a rectangular cell, the inside of which was 80-mm wide, 112.7-mm high and 160-mm deep, and a short cylinder, 106.3 mm ID and 69 mm length. The cylinder was welded onto a 36-mm thick side wall of the rectangular cell, in which a 106.3-mm dia. aperture had been bored, such that the aperture and the cylinder formed a single cylindrical space open to the rectangular space inside the cell. The outer end of the cylinder was closed with a thick plate having three ports, each equipped with a Swagelok connector. The port at the center of the plate was used for inserting a spray nozzle into the chamber, and the other two were used for supplying HFC-32 to the chamber from a high-pressure cylinder through a pressure-reducing valve and for connecting a pressure gauge to the chamber, respectively. The rectangular cell had a window, 80-mm wide and 90-mm high, on both the front and rear walls. A cylindrical brass block, 49 mm in dia. and 103 mm in length, was inserted, together with its 5.75-mm thick Teflon sheath, into the rectangular cell through its side wall opposite to the one through which the spray nozzle was inserted. The block was located such that its central axis coincided with that of the spray nozzle, and that its front surface protruded from the inside face of the cell wall by 8 mm. The brass block was tightly attached to the cell with a flange-like device. The rear side of the block was covered by a cylindrical vessel through which a temperature-controlled coolant (an aqueous ethylene glycol solution) could be circulated in such a way that the coolant was vertically injected onto the rear surface of the brass block, taking the form of a cylindrical submerged jet, and flowed out of the vessel through the two exits on its side wall. A cylindrical

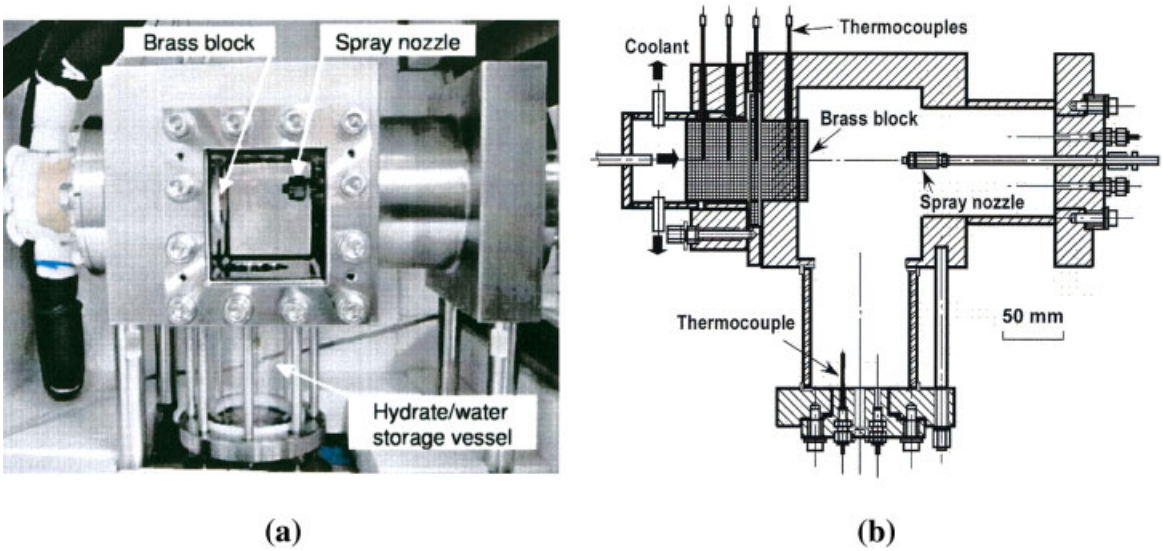

Figure 1. Outside (a), and internal structure (b) of the spray chamber integrated with a cylindrical brass block, a wall-jet cooling assembly at the rear of the brass block, and a hydrate storage vessel.

[Color figure can be viewed in the online issue, which is available at www.interscience.wiley.com.].

Pyrex vessel, 65.4 mm ID and 100 mm high, hung from the bottom of the rectangular cell. It was expected that the hydrate formed on the brass-block surface, as well as the liquid water having not converted into the hydrate fell into this vessel, and were stored there in the form of a hydrate/water two-phase pool. A 1/4-in. port on the flange-type stainless-steel bottom plate of this hydrate/water storage vessel allowed only liquid water to flow out.

Figure 2 illustrates the layout of the entire experimental system. The spray chamber and the water circulation loop were enclosed in a booth temperature-controlled at 10 ± 2 °C. The water circulation loop incorporated a nonpulsating double-plunger pump (Nihon Seimitsu Kagaku Co., model NP-KX-700), a tubular heat exchanger immersed in a water bath which was temperature-controlled by an immersion cooler and a PID-controlled heater + stirrer unit, and the aforementioned spray nozzle. This loop allowed water to be sprayed at a constant flow rate and at a constant temperature. The length of the tubular heat exchanger was determined such that the exit temperature of the internal water flow could satisfactorily approach the temperature in the bath. The water-supply line from the heat exchanger to the spray chamber was insulated so that we could regard the temperature in the bath as the temperature T_w at which the water was sprayed into the chamber. Because the loop was closed and the water in the loop was repeatedly stored in the spray chamber together with the hydrate, it is reasonable to assume that HFC-32 was constantly dissolved in the water almost up to the concentration at which the water (to be more exact, the water-rich liquid) could be equilibrated with the hydrate. This means that the net absorption of HFC-32 into the water hardly occurred during each hydrate-forming experimental run and that the consumption of HFC-32 measured during the run is ascribable to the hydrate formation.

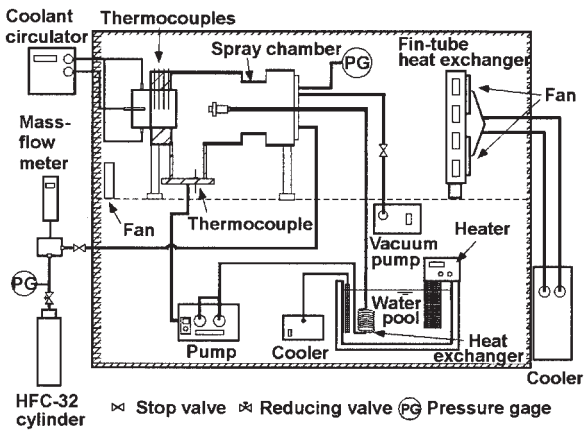

Figure 2. Experimental system layout.

The gas supply line connecting a high-pressure HFC-32 cylinder to the spray chamber was equipped with a pressure-reducing valve and a mass-flow meter (STEC SEF-V111DM + FI-1000), with which $\dot{V}_g$, the volume flow rate of HFC-32 [converted to the normal temperature—pressure condition (NTP), that is, 0 °C and 0.1013 MPa] into the spray chamber, could be measured with the uncertainty of ±0.08 cm^3/s. The pressure p inside the spray chamber was measured by a strain-gauge pressure transducer (Valcom model VPMC-D-A) with the uncertainty of ±1.5 kPa.

The spray nozzle that we used was the same flat-spray nozzle (model TP-150017 manufactured by Spraying Systems Co., Tokyo) that Fukumoto et al. used in their previous study.[9] This nozzle was so designed as to generate a flat-fan-shaped spray with an opening angle of 15 ° when the water flow rate through the nozzle was adjusted to 0.833 cm^3/s (50 cm^3/min). The Sauter mean diameter and the initial velocity of the droplets in the spray at this flow rate were 125 μm and 15.1 m/s, respectively.[9] The location and orientation of the nozzle were adjusted such that its tip was 50 mm away from the surface of the brass block, and that the spray issuing from the nozzle was horizontally spread.

Table 1. The Capacity of Heat Discharge via the Water Circulation Loop, $\dot{Q}_{w,\max}$, and that via the Brass Block with its Rear Side being Cooled by the Impinging Jet of a Coolant, $\dot{Q}_{b,\max}$

p (MPa)	T_{eq} (°C)[a]	T_w (°C)	$\Delta T_{sub,w}$ (K)	T_c (°C)	$\Delta T_{sub,c}$ (K)	$\dot{Q}_{w,\max}$ (W)	$\dot{Q}_{b,\max}$ (W)
0.410	8.6	1.5	7.1	0.5	8.1	24.9	14.5
		6.5	2.1	0.5	8.1	7.3	14.5
				5.0	3.6	7.3	6.5
0.710	13.7	6.5	7.2	0.5	13.2	25.2	23.7
				5.0	8.7	25.2	15.6
		12.0	1.7	0.5	13.2	5.9	23.7
				5.0	8.7	5.9	15.6

[a]Calculated using the correlation prepared by Akiya et al. [12] (see Appendix).

Four sheathed type-T (copper−constantan) thermocouples were inserted into the brass block normal to its axis. They were aligned at 20 mm intervals along the axis of the block to allow us to evaluate the axial temperature gradient in the block, and, thereby, to deduce the conductive heat flow rate through the block. The reason why we selected brass as the material of the block was to ensure a reasonable accuracy in determining the temperature gradient and the heat flow rate. If the block was made of copper having a much higher thermal conductivity than brass, the axial temperature gradient would be significantly reduced, resulting in a lower accuracy in determining the heat flow rate. Although copper was preferable to brass for the purpose of effectively discharging heat from any hydrate-forming system, it was not suitable for this study in which we intended to obtain a quantitative understanding of the thermal energy flow in the system.

Procedure of hydrate-forming experiments

Each experimental run was commenced by evacuating the spray chamber, water circulation loop, and the HFC-32 gas supply line between the pressure reducing valve and the spray chamber. Deionized and distilled water in the amount of 200 cm^3 was then sucked into the Pyrex hydrate/water storage vessel at the bottom of the chamber. HFC-32 (99.9% certified purity, supplied by Asahi Glass Co.) was supplied into the chamber such that the pressure in the chamber was held almost constant at the prescribed level, which was either 0.410 MPa or 0.710 MPa. The supply of HFC-32 was continued in order to compensate for the dissolution of HFC-32 into the water in the hydrate/water storage vessel. The temperature in the water bath in which the heat exchanger on the water circulation loop was immersed was controlled at a prescribed level T_w, which was 1.5, 6.5 or 12.0°C. The coolant temperature-controlled at 0.5°C or 5.0°C was circulated to chill the brass block. After the temperatures detected by the four thermocouples inserted into the block had become constant, the plunger pump on the water circulation loop was started such that water was sprayed into the chamber at the flow rate of 0.833 cm^3/s. From this time on, the rate of supply of HFC-32 into the spray chamber $\dot{V}_g$, and the temperatures in the brass block were continuously measured. At the same time, the inside of the chamber was continuously video-recorded to observe the behavior of formation and accumulation of the hydrate inside the chamber.

Evaluation of heat discharge capacity and relevant thermal quantities

The experimental hydrate-forming system outlined earlier was equipped with two devices for discharging the heat released by the hydrate formation; that is, the water circulation loop incorporating an external heat exchanger and the back-side-cooled brass block exposed to the water spray. The capacity of heat discharge for each of these devices is evaluated later.

The maximum rate of heat discharge by the water circulation loop $\dot{Q}_{w,\max}$, may be evaluated as follows[1]

$$\dot{Q}_{w,\max} = \dot{V}_w \rho_w c_{p,w} \Delta T_{sub,w} \tag{1}$$

where, $\dot{V}_w$, ρ_w and $c_{p,w}$ are the volume flow rate (= 0.833 cm^3/s), the mass density and the specific heat capacity, respectively, of the circulating water, and $\Delta T_{sub,w}$ is the degree of subcooling of sprayed water given by $T_{eq} - T_w$. The rate of heat discharge through the brass block could be controlled by the temperature T_c, and the flow rate $\dot{V}_c$ of the coolant (27.4 wt % aqueous ethylene-glycol solution) jetted onto the rear surface of the block through a tubular nozzle of 8 mm ID. During each experimental run, T_c was held constant at either of the two levels, 0.5 °C or 5.0 °C. The flow rate $\dot{V}_c$ was fixed at 41.7 cm^3/s in every run. The coefficient of convective heat transfer from the rear surface of the block to the coolant h_c, was estimated, with the aid of empirical correlations for a single round jet impinging upon a flat solid surface, to be 5.7 kW/m^2 K. (Eqs. 4.10 and 4.11a given in the review of Martin [10] were used.) Assuming a steady one-dimensional (1-D) heat transfer from the front-side surface of the brass block to the coolant on the opposite side, we can estimate the possible maximum of the heat flow rate $\dot{Q}_{b,\max}$, as follows

$$\dot{Q}_{b,\max} = \frac{1}{4} \pi D_b^2 U \Delta T_{sub,c} \tag{2}$$

where D_b is the diameter of the block (= 49 mm), $\Delta T_{sub,\,c} = T_{eq} - T_c$, and U is the overall heat-transfer coefficient. Because the thermal resistance inside the block, and that in the impinging jet flow of the coolant are connected in series, we may evaluate U as follows

$$\frac{1}{U} = \frac{L_b}{k_b} + \frac{1}{h_c} \tag{3}$$

where L_b and k_b are the axial length (= 100 mm) and the thermal conductivity (= 0.114 kW/m K), respectively, of the brass block. The values of $\dot{Q}_{w,\max}$ and $\dot{Q}_{b,\max}$ under some $p/T_w/T_c$ conditions are exemplified in Table 1. These values may be compared to the relevant values of $\dot{Q}_h$, the rate of heat

Table 2. Summarized Data of Operational Conditions and Measured Gas-Uptake Quantities

Run No.	p (MPa)	T_{eq} (°C)	T_w (°C)	$\Delta T_{sub,w}$ (K)	T_c (°C)	$\Delta T_{sub,c}$ (K)	V_{gt} (cm^3 NTP)	$\dot{V}_{g,av}$ (cm^3/s NTP)
4-1	0.408	8.5	1.5	7.0	0.5	8.0	4885	3.323
4-2	0.408	8.5	1.5	7.0	0.5	8.0	3979	2.211
4-3	0.418	8.7	6.5	2.2	0.5	8.2	1825	0.780
4-4	0.409	8.5	6.5	2.0	0.5	8.0	2274	1.263
4-5	0.414	8.6	6.5	2.1	5.0	3.6	1521	0.905
4-6	0.718	13.8	6.5	7.3	0.5	13.3	3453	3.817
4-7	0.698	13.5	6.5	7.0	0.5	13.0	2926	4.064
4-8	0.720	13.8	6.5	7.3	0.5	13.3	5878	4.898
4-9	0.698	13.5	6.5	7.0	5.0	8.5	2196	4.306
4-10	0.712	13.7	6.5	7.2	5.0	8.7	4067	3.081
4-11	0.711	13.7	6.5	7.2	5.0	8.7	1193	2.651
4-12	0.713	13.8	12.0	1.8	0.5	13.3	3580	1.989
4-13	0.711	13.7	12.0	1.7	5.0	8.7	3236	2.201

release due to the hydrate formation inside the spray chamber, and $\dot{Q}_b$, the actual rate of heat flow through the brass block, in order to evaluate the efficiency of the heat-discharge devices. The value of $\dot{Q}_b$ at each instant was deduced from the axial temperature gradient in the brass block, which was determined by applying a linear regression analysis to the instantaneous temperatures measured by the four thermocouples inserted in the brass block. The instantaneous value of $\dot{Q}_h$ was deduced from $\dot{V}_g$, the volume flow rate (at NTP) of HFC-32 into the spray chamber, as follows

$$\dot{Q}_h = (\dot{V}_g/\tilde{v}_g)\tilde{h}_{hg} \tag{4}$$

where $\tilde{v}_g$ is the molar volume of HFC-32 at NTP, and $\tilde{h}_{hg}$ is the heat of dissociation of the HFC-32 hydrate (per mole of HFC-32) under the system pressure. The value of $\tilde{v}_g$ was calculated, using the compressibility factor of HFC-32 at NTP, [11] to be 22.026×10^3 cm^3/mol. The evaluation of $\tilde{h}_{hg}$ is described in the Appendix.

Results and Discussion

Experimental conditions

The operating conditions for each experimental run are specified by the pressure inside the spray chamber (p), the temperature of water before spraying (T_w), and the temperature of the coolant impinging upon the back side of the brass block (T_c). The conditions set in each of the 13 runs performed in this study are summarized in Table 2. Each of the three operational parameters — p, T_w and T_c — were alternatively adjusted at two or three different levels in these experimental runs: that is, $p \approx 0.41$ or 0.71 MPa, $T_w = 1.5$, 6.5 or 12.0 °C, and $T_c = 0.5$ or 5.0 °C.

It should be noted that T_c is not an intrinsic parameter concerning the cooling through the brass block. In fact, the axial heat flux through the block is dependent not only on T_c, but also on such experimental parameters as h_c, k_b and L_b (see Eqs. 2 and 3) in addition to the unpredictable coefficient of heat

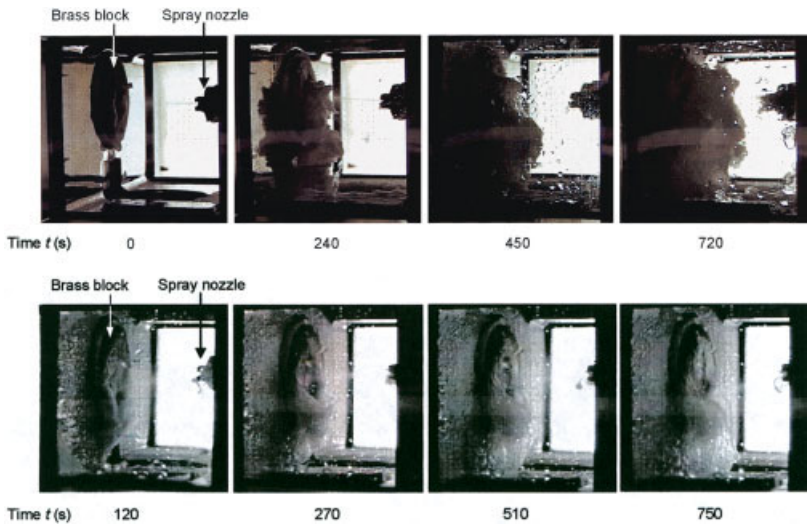

Figure 3. Sequential videographs of the formation of HFC-32 hydrate by water spraying onto the brass block surface.

Time t denotes the elapsed time after the start of water spraying.(a) Run 4-8, $p = 0.720$ MPa, $T_w = 6.5$ °C ($\Delta T_{sub,w} = 7.3$ K), $T_c = 0.5$ °C ($\Delta T_{sub,c} = 13.3$ K), and (b) Run 4-13, $p = 0.711$ MPa, $T_w = 12.0$ °C ($\Delta T_{sub,w} = 1.7$ K), $T_c = 5.0$ °C ($\Delta T_{sub,c} = 8.7$ K). [Color figure can be viewed in the online issue, which is available at www.interscience.wiley.com.].

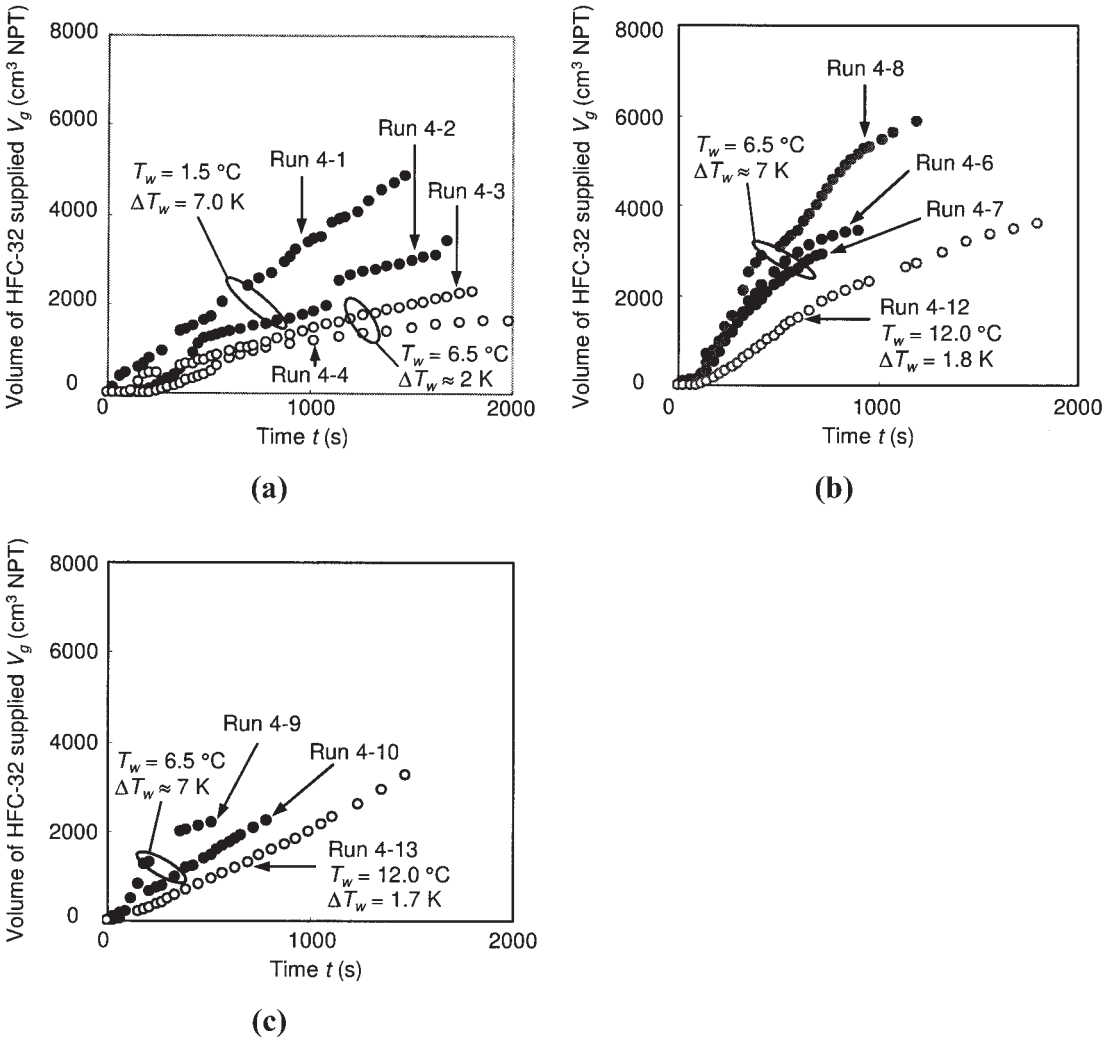

Figure 4. Time evolution of V_g, the cumulative volume (NTP) of HFC-32 supplied to the spray chamber after the first appearance of hydrate crystals, in 11 experimental runs, which are classified into three groups on the basis of the two operational parameters, p and T_c.

(a) p = 0.408–0.418 MPa, T_c = 0.5 °C ($\Delta T_{sub,c}$ = 8.0–8.2 K); (b) p = 0.698–0.720 MPa, T_c = 0.5 °C ($\Delta T_{sub,c}$ = 13.0–13.3 K), and (c) p = 0.698–0.712 MPa, T_c = 5.0 °C ($\Delta T_{sub,c}$ = 8.5–8.7 K).

transfer from the sprayed water and the hydrate slurry to the front surface of the block. Thus, T_c is no more than an apparatus-dependent parameter with which we may relatively measure the capacity of heat discharge through the brass block within the confines of the present experiments.

During each run, the pressure p exhibited some fluctuation depending on the chronological variation in the rate of hydrate formation. Once the hydrate formation started, p tended to decrease by 0.02 MPa at most, then gradually recovered toward its initial level. The decrease in the gas/water/hydrate three-phase equilibrium temperature T_{eq} corresponding to the 0.02-MPa decrease in p is 0.27 K when $p \approx 0.71$ MPa and 0.46 K when $p \approx 0.41$ MPa. (As for the $p - T_{eq}$ relation for the HFC-32/water system, consult the Appendix.) The p values indicated in Table 2, as well as in some figures shown later represent the initial pressures just before the inception of hydrate formation in the respective experimental runs.

Qualitative observations

Figure 3 shows two typical sequences of hydrate formation at nearly the same p levels — one observed at lower levels of T_w and T_c, and the other at higher levels of T_w and T_c. Regardless of the levels of T_w and T_c, we generally observed that the sprayed water turned into a hydrate slurry on the surface of the brass block. This slurry partly flowed down into the hydrate/water storage vessel below the rectangular cell and partly stuck on the surface of the brass block forming a crumbly or mushy pile on it. The visual observations indicated that the fluidity of the hydrate slurry formed on the block surface was significantly dependent on $\Delta T_{sub,w}$ and $\Delta T_{sub,c}$. When both $\Delta T_{sub,w}$ and $\Delta T_{sub,c}$ were large ($\Delta T_{sub,w} \approx 7$ K and $\Delta T_{sub,c} \approx 13$ K), the fluidity of the slurry was so low that it formed a bulky pile on the block surface within a few minutes after the start of water spraying (see sequence (a) in Figure 3). However, this pile did

not grow as to fill the space between the brass block and the spray nozzle. Generally, the pile repeated the sequence of growth and collapse, resulting in intermittent dropping of the hydrate masses from the block surface. The fluidity tended to increase with a decrease in either $\Delta T_{\mathrm{sub},w}$ or $\Delta T_{\mathrm{sub},c}$, or with decreases in both of them. When $\Delta T_{\mathrm{sub},w} \approx 2$ K and/or $\Delta T_{\mathrm{sub},c}$ was less than $\approx$9 K, the hydrate slurry continuously flowed down from the brass block surface into the hydrate/water storage vessel below it, leaving a relatively small amount of a mushy hydrate/water complex on the block surface.

Although the filling of the space between the brass block and the spray nozzle by the growing hydrate phase was successfully prevented as a result of providing the spray chamber with a sufficient hydrate-storage space below the block, the spray nozzle was still subjected to the risk of plugging due to hydrate formation on its outer surface. This was caused by the mist of water which was generated by the impingement of the water spray onto the brass block surface and filled the gas phase inside the spray chamber. The outer surface of the spray nozzle was exposed to the mist that drifted back from the brass block surface, and, hence, readily wetted by water. The water film covering the outer surface of the nozzle turned into a hydrate layer, which grew, with the aid of continuous water supply from the mist, into icicle-like lumps. The hydrate growth at the tip of the nozzle produced an instability in the water spraying and finally plugging of the nozzle. In every experimental run, the nozzle plugging occurred within 2,000 s after the start of the water spraying. Some device to prevent the nozzle tip from wetting by the water mist is required in order to further lengthen the period of each hydrate-forming operation.

Quantitative representation of experimental results

Figure 4 shows the time evolution of V_g, the cumulative volume (NTP) of HFC-32 supplied to the spray chamber after the first appearance of hydrate crystals, in each experimental run. The V_g vs. t data obtained from 11 runs were classified into three groups depending on the p and T_c levels set in these runs. (The data obtained in the residual two runs are omitted for graphical simplicity.) In general, the V_g vs. t relations were smooth and nearly linear when both $\Delta T_{\mathrm{sub},w}$ and $\Delta T_{\mathrm{sub},c}$ were small ($\Delta T_{\mathrm{sub},w} \approx 2$ K and $\Delta T_{\mathrm{sub},c} \approx 8$–9 K), and, hence, the hydrate slurry formed on the brass block surface was not heavily piled on it. More rapid increases in V_g with time t were observed when either $\Delta T_{\mathrm{sub},w}$ or $\Delta T_{\mathrm{sub},c}$ or both of them were larger. The data collected in Figure 4b (that is, the data obtained at the larger level of $\Delta T_{\mathrm{sub},c}$) show the common tendency of $\dot{V}_g$ ($\equiv dV_g/dt$) to decrease with t. This is ascribable to the growth on the brass block surface of a hydrate pile serving as an additional thermal resistance to the heat discharge to the back side of the block. A quasi-periodical alternation of the lower $\dot{V}_g$ periods and the higher $\dot{V}_g$ periods was observed in some runs (Runs 4-1, 4-2 and 4-8) operated at the larger level of $\Delta T_{\mathrm{sub},w}$ ($\approx$ 7 K). Such an alternation was confirmed to be in synchronism with the visually observed growth and collapse of a hydrate pile on the brass block surface, and, hence, it is reasonably ascribed to the fluctuation in the thermal resistance added by the hydrate pile.

The right-most data point for each experimental run shown in Figure 4 indicates the final value of V_g obtained with the regular water-spraying behavior. With more time, the spray

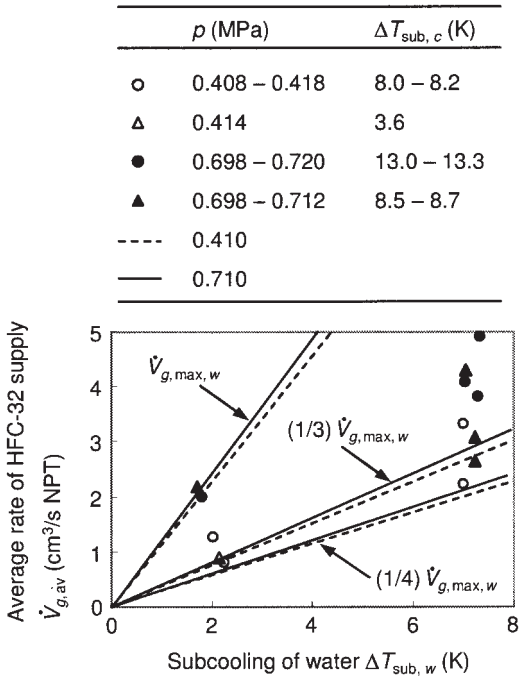

Figure 5. Dependence of the average rate of HFC-32 supply to the spray chamber $\dot{V}_{g,\mathrm{av}}$, on the subcooling of water pumped to the spray nozzle, $\Delta T_{\mathrm{sub},w}$.

The experimental $\dot{V}_{g,\mathrm{av}}$ data are compared with $\dot{V}_{g,\mathrm{max},w}$, the rate of HFC-32 supply that would be available when $\dot{Q}_h$, the rate of heat release by the hydrate formation, balances with $\dot{Q}_{w,\mathrm{max}}$, the capacity of heat discharge by water circulation.

became increasingly unstable due to the hydrate growth at the tip of the nozzle. Therefore, we specified the duration of steady water spraying till the instant corresponding to the right-most data point as the *steady spray period* τ, and defined the total volume of HFC-32 supplied to the spray chamber as $V_{g\tau} \equiv V_g$ at $t = \tau$. We further defined $\dot{V}_{g,\mathrm{av}}$, the average rate of HFC-32 supply to the spray chamber during this period, as $\dot{V}_{g,\mathrm{av}} \equiv V_{g\tau}/\tau$. The data of $V_{g\tau}$ and $\dot{V}_{g,\mathrm{av}}$, thus determined for all of the 13 experimental runs are indicated in Table 2. The $\dot{V}_{g,\mathrm{av}}$ data are also plotted versus $\Delta T_{\mathrm{sub},w}$ and $\Delta T_{\mathrm{sub},c}$ in Figures 5 and 6, respectively. In either of these figures, the $\dot{V}_{g,\mathrm{av}}$ data are sorted into four classes (as denoted by the different symbols), depending on the levels of p and $\Delta T_{\mathrm{sub},c}$ or $\Delta T_{\mathrm{sub},w}$. In each class, the data are substantially scattered (to the extent of $\pm$25% at most) presumably due to the fortuity of the growth and collapse of the hydrate piles on the brass block surface. In Figure 5, the $\dot{V}_{g,\mathrm{av}}$ data are compared with $\dot{V}_{g,\mathrm{max},w}$, the rate at which HFC-32 would be consumed by such a hydrate formation as to release heat at the rate just balancing with $\dot{Q}_{w,\mathrm{max}}$ given by Eq. 1, which is calculated as follows

$$\dot{V}_{g,\mathrm{max},w} = \tilde{\nu}_g(\dot{Q}_{w,\mathrm{max}}/\tilde{h}_{hg}) \tag{5}$$

As demonstrated elsewhere,[1] the $\dot{V}_{g,\mathrm{av}}$ data obtained in the previous studies of hydrate formation from methane by water spraying under pressures from 3.7 to 8.1 MPa [6, 7] are approximated by one-fourth or one-third of the corresponding values of $\dot{V}_{g,\mathrm{max},w}$ over the range of $\Delta T_{\mathrm{sub},w}$ from 1 to 10 K. Despite

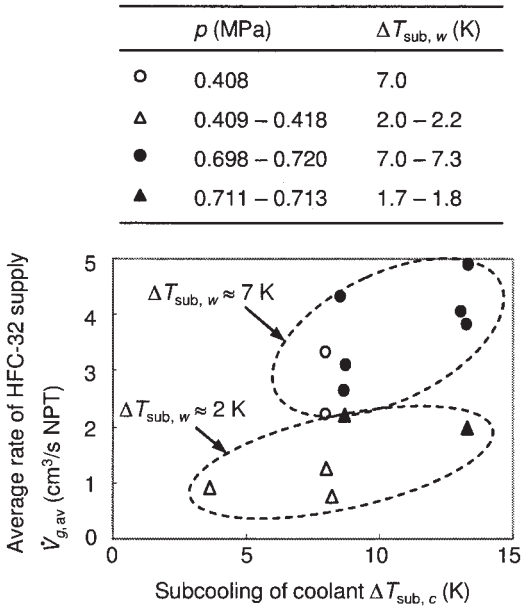

Figure 6. Dependence of the average rate of HFC-32 supply to the spray chamber $\dot{V}_{g,av}$, on $\Delta T_{sub,c}$, the temperature deficiency of the coolant for cooling the brass block from T_{eq}, the gas/water/hydrate three-phase equilibrium temperature.

the difference in the hydrate-guest species from those studies, the lower border of our $\dot{V}_{g,av}$-data group also matches with the range from one-fourth to one-third of the corresponding values of $\dot{V}_{g,max,w}$. The majority of our $\dot{V}_{g,av}$ data substantially exceed the above range, indicating the effectiveness of the cooling through the brass block in increasing the rate of hydrate formation, or the ratio of conversion of the circulated water to the hydrate, under a given water-circulation condition. On the other hand, the increase in $\dot{V}_{g,av}$ with an increasing $\Delta T_{sub,c}$, as recognized in Figure 6, is not very sharp. We cannot expect more than a twofold increase in $\dot{V}_{g.av}$ as the result of a 10-K increase in $\Delta T_{sub,c}$ from, for example, ≈5 K to ≈15 K. Such a low sensitivity of $\dot{V}_{g,av}$ to $\Delta T_{sub,c}$ is ascribable to the significant thermal resistance, to the heat flow into the brass block, placed inside the spray chamber; this is explained later.

The time evolution of some quantities related to the generation and discharge of heat during some experimental runs are shown in Figure 7. The quantities are the rate of heat release due to hydrate formation ($\dot{Q}_h$), the rate of heat discharge via the brass block ($\dot{Q}_b$), and the block surface temperature (T_b) which was determined by extrapolating the measured temperatures inside the block. Four runs operated under nearly the same pressures (p = 0.711–0.720 MPa), but for different combinations of T_w and T_c are selected. We note the most extensive fluctuation of $\dot{Q}_h$ in Runs 4-8 in which both $\Delta T_{sub,w}$ and $\Delta T_{sub,c}$ were large, and, hence, the formed hydrate slurry having a low fluidity repeated the growth and collapse of a bulky pile on the brass block surface. The least fluctuation of $\dot{Q}_h$ was exhibited in Runs 4-13, in which both $\Delta T_{sub,w}$ and $\Delta T_{sub,c}$ were small. The magnitude of $\dot{Q}_b$ in every run is found to be very small compared to the relevant value of $\dot{Q}_{b,max}$ indicated in Table 1. The ratio of $\dot{Q}_b$ to $\dot{Q}_{b,max}$ is only ≈0.3 at most (in Run 4-13), and is as low as ≈0.15 in Run 4-8, in which the hydrate pile grew the most on the brass block surface. Such low values of $\dot{Q}_b/\dot{Q}_{b,max}$ are readily interpreted in view of the level of T_b. In every run, T_b is much closer to T_c than to T_{eq} (= 13.7–13.8 K in the four runs shown in Figure 7). Obviously, the major thermal resistance to the heat flow from the hydrate-formation site to the coolant impinging on the rear side of the brass block lies neither in the block itself, nor in the coolant flow, but inside the spray chamber — more specifically, inside the hydrate/water/gas mixture resting or sliding on the brass block surface. As a result of this thermal resistance, $\dot{Q}_b$ remained at much lower levels than $\dot{Q}_h$ throughout the runs in which $\Delta T_{sub,c}$ was large (≈ 7 K), while $\dot{Q}_b$ approximately compared with $\dot{Q}_h$ in the runs in which $\Delta T_{sub,c}$ was small (≈ 2 K). In order to reduce the thermal resistance, to increase $\dot{Q}_b$, and, thereby, further increase $\dot{V}_g$ (or $\dot{Q}_h$), we need some device (or means) to promote the clearing of the hydrate slurry from the brass block surface.

Concluding Remarks

This study has revealed the potential utility of an unconventional version of the water spraying technique for hydrate formation: water spraying onto the surface of a continuously cooled metal block (or slab) inserted into a spray chamber (a hydrate reactor). Based on the series of hydrate-forming experiments performed in this study, we can conclude that the rate of hydrate formation can be significantly increased by the simultaneous use of cooling by the metal block, and that by the

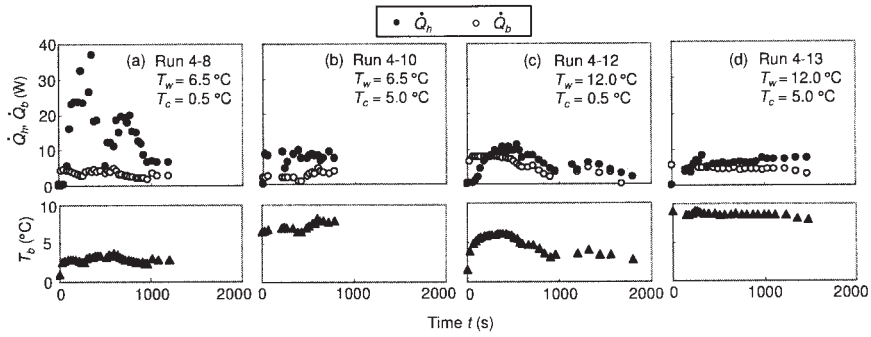

Figure 7. Simultaneous variations in the rate of heat release due to hydrate formation ($\dot{Q}_h$), the rate of heat removal via the brass block ($\dot{Q}_b$), and the block surface temperature (T_b) during the hydrate-forming experiments at p = 0.711–0.720 MPa (T_{eq} = 13.7–13.8 K).

water circulation through an external loop incorporating a heat exchanger, without overly intensifying the latter cooling at the risk of loop obstruction due to internal hydrate formation. However, two technical problems were recognized in this study and left for future investigations: (a) the plugging of the spray nozzle by hydrate formation on the nozzle tip due to water mist drifting back from the metal block surface, and (b) the growth of a wet but sticky hydrate layer on the metal block surface, hindering the heat flow into the block. Problem (a) needs to be solved to ensure long-term stable hydrate-forming operations. Problem (b) is desired to be solved in order to make the heat discharge across the metal block sufficiently effective without using an excessively cold coolant to chill the block in order to overcome the thermal resistance of the hydrate layer covering the block surface.

Acknowledgment

We thank Kuniyoshi Watanabe, student in the Dept. of Mechanical Engineering, Keio University, for his help in preparing this article.

Notation

a = constant in Eq. A1, K
b = constant in Eq. A1
c_p = specific heat capacity under constant pressure, J kg^{-1}
h_c = convective heat-transfer coefficient relevant to impinging coolant jet, W m^{-2} K^{-1}
$\tilde{h}_{hg}$ = heat of hydrate dissociation, J mol^{-1}
k_b = thermal conductivity of brass block, W m^{-1} K^{-1}
L_b = axial length of brass block, m
p = pressure inside spray chamber, Pa
$\dot{Q}_b$ = conductive heat-flow rate through brass block, W
$\dot{Q}_h$ = rate of heat release by hydrate formation, W
$\dot{Q}_w$ = rate of heat discharge by water circulation, W
$\tilde{R}$ = universal gas constant, J mol^{-1} K^{-1}
t = time lapse after the inception of hydrate formation, s
T = temperature, K or °C
T_b = temperature at front surface of brass block, K or °C
T_c = temperature of coolant, K or °C
T_{eq} = gas/water/hydrate three-phase equilibrium temperature, K or °C
T_w = temperature in water bath (≈ temperature at which water is sprayed), K or °C
U = overall heat-transfer coefficient for heat flow through brass block and coolant jet, W m^{-2} K^{-1}
$\tilde{v}_g$ = molar volume of hydrate-guest gas at NTP, m^3 mol^{-1}
V_g = accumulated volume at NTP of guest gas supplied to spray chamber after the inception of hydrate formation, m^3
$V_{g\tau}$ = V_g at $t = \tau$, m^3
$\dot{V}$ = volume flow rate (at NTP for gas), m^3 s^{-1}
Z = compressibility factor of hydrate-guest gas

Abbreviation

NTP = normal temperature and pressure, 0 °C and 0.1013 MPa

Greek letters

ΔT_{sub} = degree of subcooling (magnitude of temperature deviation from T_{eq}), K
ρ = mass density, kg m^{-3}
τ = t at the end of the period in which water spraying is not hindered by hydrate growth, s

Subscripts

av = average over the period from $t = 0$ to $t = \tau$
c = coolant
g = hydrate-guest gas
max = theoretical maximum
w = water

Literature Cited

1. Mori YH. Recent advances in hydrate-based technologies for natural gas storage — a review. *J Chem Ind Eng (China)*. 2003;54(Suppl.): 1-17.
2. Tsuji H, Ohmura R, Mori YH. Forming structure-H hydrates using water spraying in methane gas: effects of chemical species of large-molecule guest substances. *Energy & Fuels*. 2004;18:418-424.
3. Rogers R, Yevi GY, Swalm M. Hydrates for storage of natural gas. Proc 2nd Int Conf on Natural Gas Hydrates, Toulouse, France, June 2−6; 1996;423-429.
4. Yoshikawa K, Kondo Y, Kimura T, Fujimoto T. Method and device for producing hydrates (in Japanese). Patent Abstracts of Japan, Publication No. 2000-264851.
5. Nagamori S, Ono J, Nagata K. Device for continuously producing gas hydrates (in Japanese). Patent Abstracts of Japan, Publication No. 2000-264852.
6. Miyata K, Okui T, Hirayama H, Ihara M, Yoshikawa K, Nagayasu H, Iwasaki S, Kimura T, Kawasaki T, Kikuchi K, Terasaki D. A challenge to high-rate industrial production of methane hydrate. *Proc 4th Int Conf on Gas Hydrates*, Yokohama, Japan, May 19−23; 2002;1031-1035.
7. Ohmura R, Kashiwazaki S, Shiota S, Tsuji H, Mori YH. Structure-I and structure-H hydrate formation using water spraying. *Energy & Fuels*. 2002;16:1141-1147.
8. Tsuji H, Kobayashi T, Ohmura R, Mori YH. Hydrate formation by water spraying in a methane + ethane + propane gas mixture: an attempt at promoting hydrate formation utilizing large-molecule guest substances for structure-H hydrates. *Energy & Fuels*. 2005;19:869-876.
9. Fukumoto K, Tobe J, Ohmura R, Mori YH. Hydrate formation using water spraying in a hydrophobic gas: a preliminary study. *AIChE J*. 2001;47:1899-1904.
10. Martin H, Heat and mass transfer between impinging gas jets and solid surfaces. In: Hartnett JP, Irvine TF, Jr (eds.). *Advances in Heat Transfer*, Vol. 13. New York: Academic Press; 1977:1−60.
11. Lemmon EW, McLinden MO, Huber ML. NIST reference fluid thermodynamic and transport properties database (REFPROP), Ver. 7.0. US Department of Commerce, 2002.
12. Akiya T, Shimazaki T, Oowa M, Matsuo M, Yoshida Y, Formation conditions of clathrates between HFC alternative refrigerants and water. *Int J Thermophys*. 1999;20:1753-1763.
13. Sloan ED, Jr. *Clathrate Hydrates of Natural Gases*. 2nd, ed. New York: Marcel Decker, Inc; 1998: Section 4.6.1.

Appendix: Three-Phase Equilibrium in HFC-32 + Water System and Heat of Dissociation of HFC-32 Hydrate

The data processing in this study required knowledge of the gas/water/hydrate three-phase equilibrium temperature T_{eq} at given pressures p in the HFC-32 + water system. The value of the heat of hydrate dissociation $\tilde{h}_{hg}$ for each $p-T_{eq}$ condition was also required. We determined both T_{eq} and $\tilde{h}_{hg}$ at each pressure level, utilizing the empirical phase-equilibrium correlation reported by Akiya et al. [12] and the Clausius−Clapeyron equation. The phase-equilibrium correlation is given in the following form

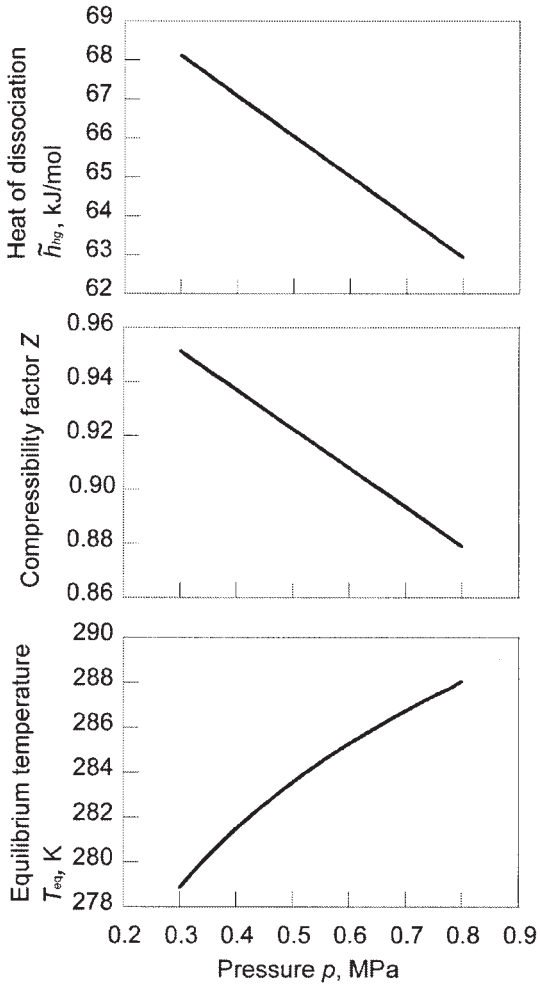

Figure A1. Pressure dependencies of the three-phase equilibrium temperature (T_{eq}), the compressibility factor of HFC-32 (Z), and the heat of hydrate dissociation per mole of HFC-32 ($\tilde{h}_{hg}$).

$$\ln\left(\frac{p}{[\mathrm{MPa}]}\right) = \frac{a}{T} + b \tag{A1}$$

where T and a are the system temperature and a curve-fitting constant, respectively, both expressed in the absolute temperature unit, K, and b is another curve-fitting constant which is dimensionless. Akiya et al. [12] determined the two constants as follows: $a = -8612.56$ K and $b = 29.681$. The equilibrium temperature T_{eq} corresponding to the level of p in each experimental run was determined as T satisfying Eq. A1.

The Clausius–Clapeyron equation relevant to the gas/water/hydrate three-phase equilibrium may be written in the following form [13]

$$\frac{d\ \ln(p/[\mathrm{MPa}])}{d(1/T)} = \frac{\tilde{h}_{hg}}{Z\tilde{R}} \tag{A2}$$

where $\tilde{R}$ is the universal gas constant, and Z is the compressibility factor of the guest gas (HFC-32) at each $p-T_{eq}$ condition. Substituting Eq. A1 into Eq. A2, we obtain

$$\tilde{h}_{hg} = -a\tilde{R}Z \tag{A4}$$

Figure A1 demonstrates the variations in T_{eq} given by Eq. A1, Z given by the REFPROP database [11], and $\tilde{h}_{hg}$ given by Eq. A4, depending on p in the range relevant to the hydrate-forming experiments in this study.

Manuscript received Jan. 31, 2006, and revision received Apr. 4, 2006.